Postprint of: Żak A., Krawczuk M., Assessment of flexural beam behaviour theories used for dynamics and wave propagation problems, Journal of Sound and Vibration, Volume 331, Issue 26 (2012), pp. 5715-5731, DOI: 10.1016/j.jsv.2012.07.034



# Assessment of flexural beam behaviour theories used for dynamics and wave propagation problems

A. Żak [a,*], M. Krawczuk [a,b]

[a] *Institute of Fluid-flow Machinery, Polish Academy of Sciences, Fiszera 14, 80-952 Gdansk, Poland*

[b] *Gdansk University of Technology, Faculty of Electrical and Control Engineering, Narutowicza 11/12, 80-952 Gdansk, Poland*

**Abstract**

In this work different theories of beam flexural behaviour have been discussed and compared. This analysis includes various one-, two- and three-dimensional beam behaviour theories comprising the classical one-dimensional Bernoulli, Bernoulli-Rayleigh, Timoshenko and Reddy theories, as well as various higher order and/or higher-mode theories of beam flexural behaviour developed by the authors. The dispersion curves obtained by the use of the Hamilton's principle and associated with each theory discussed in the paper have been also presented and analysed. The wide investigation programme carried out by the authors aimed to show major differences and similarities between the beam theories and to discuss various numerical aspects of their application. Great attention has been paid on properties, limitations as well as difficulties associated with the use of particular theories of beam flexural behaviour. Based on a wide program on numerical calculations the authors draw certain general conclusions that are valid not only in the field of wave propagation related problems, but also in the field of dynamics of engineering beam-like structures.

*Key words:* beam theories, dynamics, elastic wave propagation, flexural waves

* Corresponding author
*Email addresses:* a.zak@imp.gda.pl (A. Żak), mk@imp.gda.pl (M. Krawczuk).

*20 July 2012*

## 1 Introduction

As structural members beams have been used since centuries and during that long period of time beams have become one of the most fundamental elements of engineering structures. However, understanding of their structural characteristics starts only from the golden age of physics and mathematics, when the first mathematical models of their mechanical behaviour appeared. The classical beam theory, also known as the Bernoulli, Euler or Bernoulli-Euler [1] beam theory, crystallised around 1750 by complementary efforts of Bernoulli and Euler. But it remained unknown for almost one century to re-emerge during the times of the second industrial revolution and such spectacular engineering structures like the Eifel tower or Ferris wheel. Because of the extensive and universal use of beams for more advanced and sophisticated structures more accurate models of their flexural behaviour were required. As the effect of this demand new beam theories were proposed and developed such as, for example, the Rayleigh or Bernoulli-Rayleigh beam theory [2] developed at the end of the XIX-th century as an enhancement over the classical beam theory, and which incorporates the rotary inertia of the beam cross-section or the Timoshenko beam theory [3, 4] from the beginning of the XX-th century that additionally takes into account the effect of transverse shear stress. Other examples can be the higher order beam theories developed by Levinson [5] or Heyliger and Reddy [6] that assumed parabolic distribution of the shear stress over the beam cross-section.

It should be noted here that an increasing degree of accuracy of these theories in terms of their static or dynamic predictions were in fact limited because all of them were based on the simplifications of the theory of elasticity to one dimension only. These approximations may lead to incorrect solutions in more complicated or specific cases, where two- or three-dimensional nature of the beam behaviour must be taken into account. Specialised theories of thin-walled beams, such as one developed by Vlasov [7] or other theories [8, 9] based on solutions of the Saint-Venant problem [10, 11] of coupled bending-shear beam behaviour, overcome the issues mentioned before, however, at the cost of additional mathematical complications.

A special class of engineering problems related to the use of beams as structural members are the problems involving high frequency excitations and responses that on the other hand imply high velocities of propagating signals. This is typical not only in the case of various problems related with propagation of elastic waves in beam-like structures, but also in the case of their high frequency steady-state or transient dynamics. In all these cases accurate numerical modelling of beam dynamic behaviour is a key issue and its precise representation in space and time requires very dense spatial and time discretisation making the discretisation process a main and most crucial factor of the

analysis. Because of that fact many different numerical modelling techniques have been used for that purpose as well as reported in the literature.

Over last decades a big variety of numerical techniques have been developed and applied for solutions of problems related to propagation of elastic waves as well as wave interaction with damage related discontinuities. These techniques can be divided into two separate classes due to significantly different approach they employ. The first class are so-called frequency-domain methods (FD) that are based on the frequency representation of excitation signals and structural responses, which techniques inherently employ the direct and inverses fast Fourier transforms (FFT and IFFT). A good introduction to this approach was given by Doyle [12], who studied and analysed dynamic characteristics and propagation of elastic waves in typical one- and two-dimensional structural elements. Based on this approach various aspects of dynamics, wave propagation and wave-damage interaction in beam-like structures were studied and reported in [13–21]. The second class are so-called time domain methods (TD) and they include the classical finite difference (FDM) [22–25] and element (FEM) methods [26–30]. Based on the foundations laid by the frequency and time domain methods mentioned two other numerical techniques have emerged and developed that now are repeatedly used for wave propagation related problems. They are very well represented by the time-domain spectral element method or the spectral finite element method proposed by Patera [31]. The use of the spectral finite element method for investigation of propagation of elastic waves and wave-damage interaction in beam-like structures was presented and reported in [32–35] and the other branch of the time-domain methods are the methods that apply the wavelet transform in a similar manner as it takes place in the frequency-domain approach. In the case of dynamic problems related with beam-like structures they can be represented by [36–38].

It is interesting to note that the applicability of particular theories of beam flexural behaviour used by the authors of the papers mentioned above is always limited to certain frequency or loading regimes. However, this fact is not always appropriately addressed and/or very often neglected, which may lead to wrong interpretation of simulation results or even to false conclusions. Taking this into account it becomes obvious that different theories of beam flexural behaviour reported in the literature should be analysed and evaluated in a much more systematic and careful manner. For this reason in this work different theories of beam flexural behaviour have been discussed and compared. These includes various one-, two- or three-dimensional beam behaviour theories comprising the classical one-dimensional Bernoulli, Bernoulli-Rayleigh, Timoshenko and Reddy theories, as well as various higher-order and multimode theories of beam flexural behaviour developed by the authors. The dispersion curves obtained by the use of the Hamilton's principle and associated with each theory discussed in the paper have been also presented and analysed. The wide investigation programme carried out by the authors aimed to

show major differences and similarities between the beam theories and to discuss various numerical aspects of their application. Great attention has been paid on properties, limitations as well as difficulties associated with the use of particular beam behaviour theories. Based on a wide program on numerical calculations the authors draw certain general conclusions that are valid not only in the field of wave propagation related problems, but also in the field of dynamics of engineering beam-like structures.

## 2 Elastic waves in beams

### *2.1 Theoretical background*

Propagation of elastic waves in beam structural elements can be well described by the linear theory of elasticity. In the case of isotropic materials the equation of motion governing propagation of elastic waves can be expressed in a vector form as [12, 39, 40]:

$$\mu\nabla^2\boldsymbol{u} + (\lambda + 2\mu)\,\mathrm{grad}\,\mathrm{div}\,\boldsymbol{u} = \rho\,\ddot{\boldsymbol{u}} \tag{1}$$

where $\boldsymbol{u}$ is a displacement vector, $\lambda$ and $\mu$ are Lamé material elastic constants, $\rho$ denotes material density and $\ddot{\square}$ is the second time derivative.

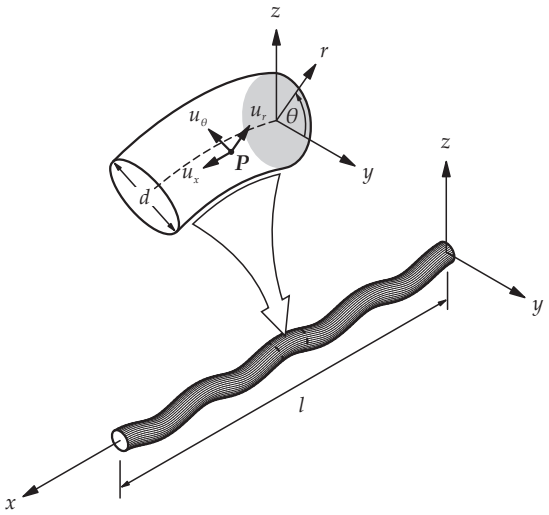


Fig. 1. Geometry of a beam structural element.

It is most convenient to analyse this problem using the cylindrical $(x, r, \theta)$ rather than the Cartesian $(x, y, z)$ coordinates – see Fig. 1. In the cylindrical coordinate system the components $u_x$, $u_r$ and $u_\theta$ of the displacement vector $\boldsymbol{u}$ are certain scalar functions of the space coordinates $x$, $r$ and $\theta$ as well as time $t$.

According to Helmholtz's theorem the field of the displacement vector $\boldsymbol{u}$ can be thought of as a sum of two special vector fields $\boldsymbol{u}_\phi$ and $\boldsymbol{u}_H$ such that the vector field $\boldsymbol{u}_\phi$ is irrotational ($\text{rot}\,\boldsymbol{u}_\phi = 0$), while the vector field $\boldsymbol{u}_H$ is solenoidal ($\text{div}\,\boldsymbol{u}_H = 0$). This is achieved by assuming that the field of the displacement vector $\boldsymbol{u}$ is generated by a pair of potentials, i.e. scalar potential $\phi$ and vector potential $\boldsymbol{H} = (H_x, H_r, H_\theta)$:

$$\boldsymbol{u} = \boldsymbol{u}_\phi + \boldsymbol{u}_H = \text{grad}\,\phi + \text{rot}\,\boldsymbol{H}, \quad \text{div}\,\boldsymbol{H} = 0 \tag{2}$$

with the following notation employed:

$$\text{grad}\,\phi = \hat{\boldsymbol{i}}\,\frac{\partial\phi}{\partial x} + \hat{\boldsymbol{r}}\,\frac{\partial\phi}{\partial r} + \hat{\boldsymbol{\theta}}\,\frac{1}{r}\frac{\partial\phi}{\partial\theta}, \quad \text{div}\,\boldsymbol{H} = \frac{\partial H_x}{\partial x} + \frac{1}{r}\frac{\partial(rH_r)}{\partial r} + \frac{1}{r}\frac{\partial H_\theta}{\partial\theta}$$

$$\text{rot}\,\boldsymbol{H} = \hat{\boldsymbol{i}}\,\frac{1}{r}\left[\frac{\partial(rH_\theta)}{\partial r} - \frac{\partial H_r}{\partial\theta}\right] + \hat{\boldsymbol{r}}\left[\frac{1}{r}\frac{\partial H_x}{\partial\theta} - \frac{\partial H_\theta}{\partial x}\right] + \hat{\boldsymbol{\theta}}\left[\frac{\partial H_r}{\partial x} - \frac{\partial H_z}{\partial r}\right]$$

$$\nabla^2 = \frac{\partial^2}{\partial x^2} + \frac{\partial^2}{\partial r^2} + \frac{1}{r}\frac{\partial}{\partial r} + \frac{1}{r^2}\frac{\partial^2}{\partial\theta^2}$$

where $\hat{\boldsymbol{i}}$, $\hat{\boldsymbol{j}}$ and $\hat{\boldsymbol{\theta}}$ are the unit vectors indicating the orientations of the $x$, $r$ and $\theta$ axes.

Application of Helmholtz's theorem and substitution of Eq.(2) into Eq.(1) leads after some simplification and rearranging of the terms related to both potentials $\phi$ and $\boldsymbol{H}$ to Eq.(3):

$$\text{grad}\left[(\lambda + 2\mu)\nabla^2\phi - \rho\frac{\partial^2\phi}{\partial t^2}\right] + \text{rot}\left[\mu\nabla^2\boldsymbol{H} - \rho\frac{\partial^2\boldsymbol{H}}{\partial t^2}\right] = 0 \tag{3}$$

which presents in fact a set of two independent equations of motion for both potentials $\phi$ and $\boldsymbol{H}$:

$$\nabla^2\phi = \frac{1}{c_l^2}\frac{\partial^2\phi}{\partial t^2}, \quad \nabla^2\boldsymbol{H} = \frac{1}{c_t^2}\frac{\partial^2\boldsymbol{H}}{\partial t^2} \tag{4}$$

where $c_l$ and $c_t$ defined as follows:

$$c_l^2 = \frac{\lambda + 2\mu}{\rho}, \quad c_t^2 = \frac{\mu}{\rho} \tag{5}$$

denote the velocities of longitudinal (irrotational, voluminal, dilatational or primary) and torsional (rotational, equi-voluminal, shear or secondary) waves propagating in three-dimensional unbounded isotropic media, respectively.

*2.2 Characteristic frequency equation*

Using the cylindrical $(x, r, \theta)$ coordinates the components $u_x$, $u_r$ and $u_\theta$ of the displacement vector $\boldsymbol{u}$ can be related to the scalar potential $\phi$ and the components $H_x$, $H_r$ and $H_\theta$ of the vector potential $\boldsymbol{H}$ through the relations:

$$\begin{gathered} u_x = \frac{\partial \phi}{\partial x} + \frac{1}{r}\frac{\partial (r H_\theta)}{\partial r} - \frac{1}{r}\frac{\partial H_r}{\partial \theta} \\ u_r = \frac{\partial \phi}{\partial r} + \frac{1}{r}\frac{\partial H_x}{\partial \theta} - \frac{\partial H_\theta}{\partial x}, \quad u_\theta = \frac{1}{r}\frac{\partial \phi}{\partial \theta} + \frac{\partial H_r}{\partial x} - \frac{\partial H_x}{\partial r} \end{gathered} \tag{6}$$

which after substitution to Eq.(1) and some simplifications results in another set of four independent equations of motion expressed in terms of the scalar and vector potentials $\phi$ and $\boldsymbol{H}$:

$$\begin{gathered} \nabla^2 \phi = \frac{1}{c_l^2}\frac{\partial^2 \phi}{\partial t^2}, \quad \nabla^2 H_x = \frac{1}{c_t^2}\frac{\partial^2 H_x}{\partial t^2} \\ \nabla^2 H_r - \frac{H_r}{r^2} - \frac{2}{r^2}\frac{\partial H_\theta}{\partial \theta} = \frac{1}{c_t^2}\frac{\partial^2 H_r}{\partial t^2} \\ \nabla^2 H_\theta - \frac{H_\theta}{r^2} + \frac{2}{r^2}\frac{\partial H_r}{\partial \theta} = \frac{1}{c_t^2}\frac{\partial^2 H_\theta}{\partial t^2} \end{gathered} \tag{7}$$

The strain field within the beam can be easily evaluated based on Eqs.(6) and has the following components:

$$\begin{gathered} \epsilon_{xx} = \frac{\partial u_x}{\partial x}, \quad \epsilon_{rr} = \frac{\partial u_r}{\partial r}, \quad \epsilon_{\theta\theta} = \frac{u_r}{r} + \frac{1}{r}\frac{\partial u_\theta}{\partial \theta} \\ \gamma_{r\theta} = \frac{\partial u_\theta}{\partial r} - \frac{u_\theta}{r} + \frac{1}{r}\frac{\partial u_r}{\partial \theta}, \quad \gamma_{\theta x} = \frac{1}{r}\frac{\partial u_x}{\partial \theta} + \frac{\partial u_\theta}{\partial x}, \quad \gamma_{xr} = \frac{\partial u_r}{\partial x} + \frac{\partial u_x}{\partial r} \end{gathered} \tag{8}$$

while the stress field can be calculated from Hooke's law based on the following very well-known formulas:

$$\begin{gathered} \sigma_{xx} = 2\mu\epsilon_{xx} + \lambda(\epsilon_{xx} + \epsilon_{rr} + \epsilon_{\theta\theta}) \\ \sigma_{rr} = 2\mu\epsilon_{rr} + \lambda(\epsilon_{xx} + \epsilon_{rr} + \epsilon_{\theta\theta}) \\ \sigma_{\theta\theta} = 2\mu\epsilon_{\theta\theta} + \lambda(\epsilon_{xx} + \epsilon_{rr} + \epsilon_{\theta\theta}) \\ \tau_{r\theta} = \mu\gamma_{r\theta}, \quad \tau_{\theta x} = \mu\gamma_{\theta x}, \quad \tau_{xr} = \mu\gamma_{xr} \end{gathered} \tag{9}$$

Flexural harmonic waves that can propagate within the beam along its longitudinal $x$ axis can be assumed as solutions of Eqs.(7) in a general complex

form [39]:

$$\begin{aligned} \phi &= \hat{\phi}(r)\cos n\theta\, e^{i(kx-\omega t)} \\ \boldsymbol{H} &= [\hat{H}_x(r)\sin n\theta, \hat{H}_r(r)\sin n\theta, \hat{H}_\theta(r)\cos n\theta]e^{i(kx-\omega t)} \end{aligned} \tag{10}$$

where $\hat{\phi}(r)$ as well as $\hat{H}_x(r)$, $\hat{H}_r(r)$ and $\hat{H}_\theta(r)$ are unknown functions and $k$ denotes the wave number, while $\omega$ is the angular frequency, while $n$ is an integer number. It should be noted here that an infinite set of solutions can be built based on the postulated solutions, however, the most important family of these solutions is associated with $n = 1$.

Substitution of solutions (10) to the equations of motion (8) followed by certain simplifications leads to a set of Bessel's differential equations for the functions $\hat{\phi}(r)$ as well as $\hat{H}_x(r)$, $\hat{H}_r(r)$ and $\hat{H}_\theta(r)$:

$$\begin{aligned} \frac{d^2\hat{\phi}}{dr^2} + \frac{1}{r}\frac{d\hat{\phi}}{dr} - \frac{\hat{\phi}}{r^2} + \alpha^2\hat{\phi} &= 0 \\ \frac{d^2\hat{H}_x}{dr^2} + \frac{1}{r}\frac{d\hat{H}_x}{dr} - \frac{\hat{H}_x}{r^2} + \beta^2\hat{H}_x &= 0 \\ \frac{d^2\hat{H}_r}{dr^2} + \frac{1}{r}\frac{d\hat{H}_r}{dr} - \frac{2\hat{H}_r}{r^2} + \beta^2\hat{H}_r + \frac{2\hat{H}_\theta}{r^2} &= 0 \\ \frac{d^2\hat{H}_\theta}{dr^2} + \frac{1}{r}\frac{d\hat{H}_\theta}{dr} - \frac{2\hat{H}_\theta}{r^2} + \beta^2\hat{H}_\theta + \frac{2\hat{H}_r}{r^2} &= 0 \end{aligned} \tag{11}$$

where:

$$\alpha^2 = \frac{\omega^2}{c_l^2} - k^2, \quad \beta^2 = \frac{\omega^2}{c_t^2} - k^2$$

that has solutions in the form of Bessel's functions of the first kind $J_i(\alpha r)$ and $J_i(\beta r)$ as well as Bessel's functions of the second kind $Y_i(\alpha r)$ and $Y_i(\beta r)$, where $i = 0, 1, 2$. Because the second kind Bessel's functions exhibit singular behaviour at their origin at $r = 0$ this branch of the solution is discarded leading to the following form of the solution of the problem under investigation:

$$\begin{aligned} \hat{\phi}(r) = AJ_1(\alpha r), \quad \hat{H}_x(r) = BJ_1(\beta r) \\ \hat{H}_r(r) = CJ_0(\beta r) + DJ_2(\beta r), \quad \hat{H}_\theta(r) = CJ_0(\beta r) - DJ_2(\beta r) \end{aligned} \tag{12}$$

where $A$, $B$, $C$ and $D$ are certain constants.

Taking into account the general form of the solutions from Eqs.(10) it can be

finally written that:

$$\begin{aligned} \phi &= AJ_1(\alpha r)\cos n\theta\, e^{i(kx-\omega t)} \\ H_x &= BJ_1(\beta r)\sin n\theta\, e^{i(kx-\omega t)} \\ H_r &= [CJ_0(\beta r) + DJ_2(\beta r)]\sin n\theta\, e^{i(kx-\omega t)} \\ H_\theta &= [CJ_0(\beta r) - DJ_2(\beta r)]\cos n\theta\, e^{i(kx-\omega t)} \end{aligned} \tag{13}$$

Propagation of elastic flexural waves within the beam requires the fulfilment of zero-traction boundary conditions on the beam outer surface that accompany the set of the equations of motion given by Eqs.(7). They can be written in the following way:

$$\sigma_{rr}(x,a,\theta) = \tau_{r\theta}(x,a,\theta) = \tau_{xr}(x,a,\theta) = 0 \tag{14}$$

where $l$ is the length and $d = 2a$ is the diameter of the beam.

The zero-traction boundary conditions for the stress components $\sigma_{rr}$, $\tau_{r\theta}$ and $\tau_{xr}$, after substitution of Eqs.(13) to Eqs.(8) and by the subsequent use of the formulas from Eqs.(9) and some simplification, form a set of two homogeneous equations expressed in terms of the two solutions from Eqs.(13).

The given set of equations has a non-trivial solution only then when its determinant vanishes. In the case under consideration this condition leads directly to a certain non-linear equation dependant on the angular frequency $\omega$ and the wave number $k$ and independent of the angle $\theta$. This is the characteristic frequency equation for flexural (bending) modes propagating in isotropic beams and has the following form:

$$\begin{aligned} c_1 J_1(\alpha a)J_0^2(\beta a) - J_0(\beta a)J_1(\beta a)[c_2 J_0(\alpha a) + c_3 J_1(\alpha a)] + \\ J_1^2(\beta a)[c_4 J_0(\alpha a) + c_5 J_0(\alpha a)] = 0 \end{aligned} \tag{15}$$

where the coefficients $c_i (i = 1, \ldots, 5)$, are expressed based on the relations:

$$\begin{aligned} c_1 &= 2\beta a^2(\beta^2 - k^2)^2 \\ c_2 &= 2\alpha\beta^2 a^2(5k^2 + \beta^2) \\ c_3 &= a[k^2\beta^2(2 + k^2a^2) - 2\beta^4(5 + k^2a^2) + \beta^6 a^2 - 4k^4] \\ c_4 &= 2\alpha\beta a[\beta^2 + k^2(9 - 2a^2\beta^2)] \\ c_5 &= \beta(k^2 + \beta^2)[a^2(k^2 + \beta^2) - 8] \end{aligned} \tag{16}$$

*2.3 Solution of the characteristic frequency equation*

The characteristic frequency equation related with propagation of flexural elastic waves was solved by the use of an original and dedicated program written by the authors in *Matlab* environment [41]. The values of the velocities of longitudinal $c_l$ and torsional $c_t$ waves propagating within the beam were calculated assuming the beam made out of aluminium with Young's modulus $E = 72.7$ GPa, Poisson ratio $\nu = 0.33$ and material density $\rho = 2700$ kg/m$^3$ and of the diameter $d = 0.01$ m. The values of the characteristic velocities were $c_l = 6.3$ km/s and $c_t = 3.2$ km/s, respectively.

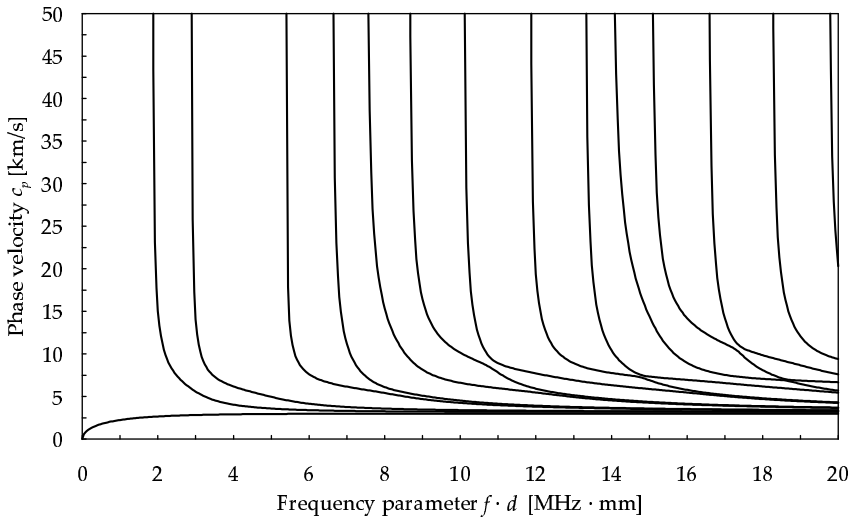


Fig. 2. Phase velocity $c_p$ dispersion curves for an aluminium beam ($c_l = 6.3$ km/s, $c_t = 3.2$ km/s).

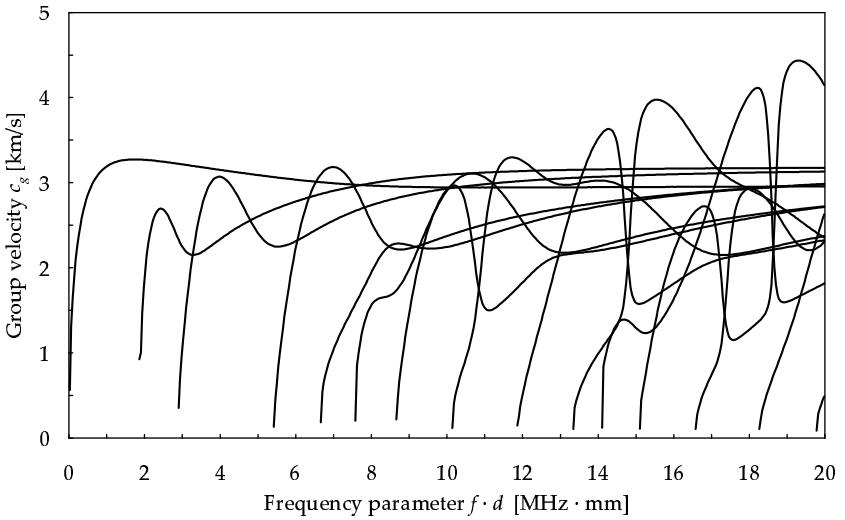


Fig. 3. Group velocity $c_g$ dispersion curves for an aluminium beam ($c_l = 6.3$ km/s, $c_t = 3.2$ km/s).

As a calculation domain the frequency range $f$ from 0.1 Hz up to 2.0 MHz and the phase velocity range $c_p$ from 2 km/s up to 50 km/s was chosen. The roots of the characteristic frequency equation were sought at nodes of a regular grid of $400 \times 2000$ nodes at the assumed accuracy level $\delta \leq 0.001\%$.

The solution was based on the use of a conjugate bisection method developed by the authors [42]. In the first step the roots were found as a function of the phase velocity $c_p = \omega/k$ for given values of the frequency $f = \omega/\pi/2$ treated as a parameter in Eq.(15). In the second step the phase velocity $c_p$ was assumed to be a parameter and the roots were found as a function of the frequency $f$. In this way the second step of calculations improved the solutions obtained from the first step for those regions of analysis where changes in the phase velocity $c_p$ as a function of the frequency $f$ were of a very high magnitude.

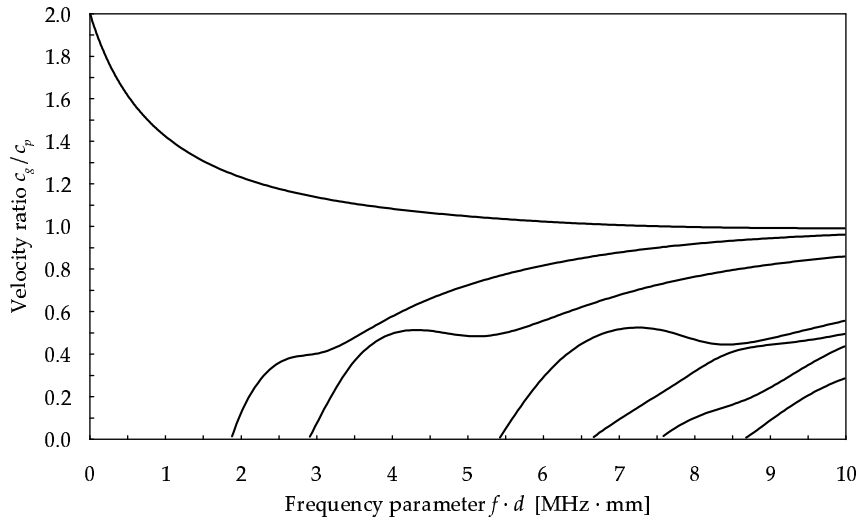


Fig. 4. Group-to-phase velocity ratio $c_g/c_p$ dispersion curves for an aluminium beam ($c_l = 6.3$ km/s, $c_t = 3.2$ km/s).

The results obtained for changes in the phase velocity $c_p$ as a function of a frequency parameter $f \cdot d$ are shown in Fig. 2, while Fig. 3 presents changes in the group velocity $c_g$ as a function of the same frequency parameter $f \cdot d$. The values of the group velocity $c_g = d\omega/dk$ were also obtained numerically by differentiation of the wave number curves $k = k(\omega)$ with respect to the angular frequency $\omega$.

However, it is very convenient to present the dispersion curves shown in Fig. 2 and Fig. 3 in such a unified or normalised manner. A typical example of such standardisation is normalisation of dispersion curves for the group velocity $c_g$ by the phase velocity $c_p$, so they express changes in the group-to-phase velocity ratio $c_g/c_p$. The dispersion curves obtained based on such normalisation for the range of the frequency parameter $f \cdot d$ up to 10 MHz·mm are presented in Fig. 4.

## 3 Beam theories

### *3.1 General considerations*

The beam theories used for various dynamic problems, also including propagation of flexural elastic waves in beam-like structures and reported in the literature, can generally be classified as one-, two- or three-dimensional theories. The nature of the stress and strain state within the structures can be considered as a key element of such classification. Although this classification is not precise, it greatly helps to differentiate and allocate particular beam theories to a right group in order to assess their properties or characteristics. Other classification can be based on a number of wave modes associated with the theories, which allows one to distinguish one-mode, two-mode, three-mode as well as higher mode theories. Additionally to that certain higher order theories can be also marked out as the theories that make use of the zero-traction boundary conditions, as specified by Eqs.(14).

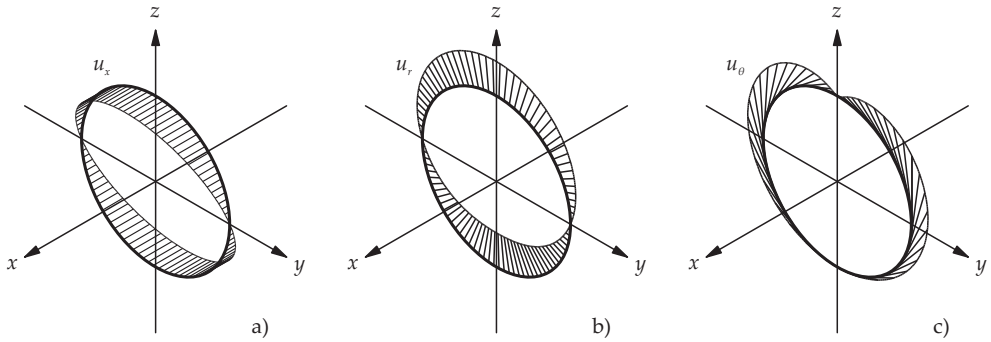


Fig. 5. Distributions of displacement components $u_x$, $u_r$ and $u_\theta$ within the circular cross-section of a beam element due to flexural behaviour: a) longitudinal displacement component $u_x$, b) radial displacement component $u_r$, c) and tangent displacement component $u_\theta$.

A great number of theories based on different forms of displacement fields can be obtained through investigation of a general three-dimensional displacement field of a beam structural element, as presented in Fig. 1 and based on Eqs.(6) and Eqs.(10). An appropriate Maclaurin series expansion enables one not only to reduce the number of unknown variables to a desired and necessary number, but it also helps to simplify the complexity of the displacement field. Cutting off the number of wave propagation modes than are allowed by particular theories limits their application range and helps one to shape the theories to specified needs or requirements.

Using the same cylindrical coordinates $(x, r, \theta)$ the displacement filed corresponding to the displacement vector $\boldsymbol{u} = [u_x, u_r, u_\theta]$ associated with flexural

behaviour of a beam structural element can be formally presented in the following general form [39, 40]:

$$\begin{aligned} u_x(x,r,\theta) &= U_x(x,r)\sin\theta \\ u_r(x,r,\theta) &= U_r(x,r)\sin\theta \\ u_\theta(x,r,\theta) &= U_\theta(x,r)\cos\theta \end{aligned} \tag{17}$$

where $U_x(x,r)$, $U_r(x,r)$ and $U_\theta(x,r)$ are certain unknown displacement functions dependant only on the spatial coordinates $x$ and $r$. Typical distributions of the displacement components $u_x$, $u_r$ and $u_\theta$ within the circular cross-section of a beam element corresponding to Eq.(17) illustrates Fig. 5.

The unknown displacement functions $U_x(x,r)$, $U_r(x,r)$ and $U_\theta(x,r)$ of the beam displacement field can be formally expanded into a Maclaurin series of the about $r = 0$ leads to the relations:

$$\begin{aligned} U_x(x,r) &= U_x(x,0) + \sum_{k=1}^{\infty} \frac{\partial^k U_x(x,0)}{\partial r^k}\frac{r^k}{k!} \\ U_r(x,r) &= U_r(x,0) + \sum_{k=1}^{\infty} \frac{\partial^k U_r(x,0)}{\partial r^k}\frac{r^k}{k!} \\ U_\theta(x,r) &= U_\theta(x,0) + \sum_{k=1}^{\infty} \frac{\partial^k U_\theta(x,0)}{\partial r^k}\frac{r^k}{k!} \end{aligned} \tag{18}$$

It is interesting to note at this place that the terms that are proportional to the odd and even values of $k$ have different meanings. In the case of the displacement function $U_x$ only the odd values of $n$ are associated with antisymmetric behaviour and propagation of flexural waves, while in the case of the displacement functions $U_r(x,r)$ and $U_\theta(x,r)$ these are the even values of $n$ [12, 39, 40].

The number of terms kept in the series given by Eqs.(18) must always depend on the investigated phenomena. It is directly related with the total number of degrees of freedom as well as the total number of wave propagation modes of a finite element approximation based on the expansion. The expansion of the displacement component $U_\theta(x,r)$ leads to the series of the following form:

$$U_\theta(x,r) = U_\theta(x,0) + \sum_{k=1}^{n} \frac{\partial^k U_\theta(x,0)}{\partial r^k}\frac{r^k}{k!} + O(r^{n+1}) \tag{19}$$

where $O(r^{n+1})$ represents the truncation error of the expansion proportional to $r^{n+1}$. A step towards a finite element approximation can be made when Eq.

(19) is rewritten as:

$$U_\theta(x,r) = \sum_{k=0}^{n} \vartheta_k(x) r^k + O(r^{n+1}) \tag{20}$$

where $\vartheta_k(x)(k = 0, 1, \ldots, n)$ denotes now degrees of freedom of a beam element associated with a Maclaurin series expansion of the displacement component $U_\theta(x,r)$.

It should be emphasised once more that the truncation of the series (18) results in an approximation error proportional to $O(r^{n+1})$. Due to this fact the formula obtained for each displacement function $U_x(x,r)$, $U_r(x,r)$ and $U_\theta(x,r)$, as presented by Eq.(20), is not exact in its representation of a fully three-dimensional displacement field. However, it should be also said that effective solutions of most of engineering problems related to various static or low-frequency dynamic problems require displacement fields that are based only on the first one or two terms of the appropriate Maclaurin series. In the case considered above it can be noted immediately that:

$$\vartheta_0(x) = U_\theta(x,0), \quad \vartheta_k(x) = \frac{1}{k!}\frac{\partial^k U_\theta(x,0)}{\partial r^k}, \quad k = 1, 2, \ldots, n \tag{21}$$

Contrary to that a great majority of problems related to high-frequency dynamics or propagation of flexural elastic waves in beam-like structures requires much more accurate representation of the three-dimensional displacement field of a solid element. Here it should be reminded that in a general case propagation of elastic waves within structural elements or wave guides is related with coupled interaction of the shear and extensional waves with structural lateral boundaries. As a consequence of this interaction propagation of various modes of flexural elastic waves can be observed. For this reason an appropriate representation of these modes in a broad range of frequencies requires a greater number of terms of Maclaurin series, given by Eqs.(18), in order to capture the complexity of the interaction phenomena [32–35].

### *3.2 Displacement fields*

Based on the previous considerations a general form of the displacement field of a beam element corresponding to the displacement vector $\boldsymbol{u} = [u_x, u_r, u_\theta]$ and associated with its flexural behaviour can be represented as:

$$\begin{aligned} u_x(x,r,\theta) &= \tilde{U}_x(x,r)\sin\theta \\ u_r(x,r,\theta) &= \tilde{U}_r(x,r)\sin\theta \\ u_\theta(x,r,\theta) &= \tilde{U}_\theta(x,r)\cos\theta \end{aligned} \tag{22}$$

where now the expansions of the displacement functions $\tilde{U}_x(x,r)$, $\tilde{U}_r(x,r)$ and $\tilde{U}_\theta(x,r)$ take the following forms:

$$\begin{aligned}\tilde{U}_x(x,r) &= \sum_{k=0}^{n} \phi_{2k+1}(x) r^{2k+1} \\ \tilde{U}_r(x,r) &= \sum_{k=0}^{n} \psi_{2k}(x) r^{2k} \\ \tilde{U}_\theta(x,r) &= \sum_{k=0}^{n} \vartheta_{2k}(x) r^{2k}\end{aligned} \tag{23}$$

with an additional condition resulting from the symmetry with respect to the bending plane $xz$, as can be seen in Fig. 5, stating that:

$$\psi_0(x) = \vartheta_0(x) \tag{24}$$

and when $3n+3$ terms of the series expansion are kept. Each particular term of the series expansions of the displacement functions $\phi_{2k+1}(x)$, $\psi_{2k}(x)$ and $\vartheta_{2k}(x)$, with $k = 0, 1, \ldots, n$, may be interpreted as an independent nodal degree of freedom. For example in the case of $n = 2$ including only three of such terms for each displacement component leads to the displacement field of a beam element having as many as eight degrees of freedom per node. This high number of the independent nodal degrees of freedom may be, however, successfully reduced down from eight to five by the use of the zero-traction boundary conditions (14). Throughout this paper all such beam theories that take advantage of these conditions, fully or partially, are consequently referred by the authors as higher order theories of beam flexural behaviour.

It should be noted that any practical application of the zero-traction boundary conditions, expressed by Eq.(14), together with the displacement field given by Eqs.(22) and Eqs.(23), results in a set of partial differential equations that are, in general, very difficult to solve. This problem can be avoided by simple substitution and rearrangement of terms [43] that leads to new forms of the displacement fields for one-, two- and three-dimensional theories of beam flexural behaviour – for clarity and simplicity of the presentation the arguments $x$ and $r$ will be omitted hereinafter:

- *Three-dimensional theories*:

$$\begin{aligned}u_x &= \left[\phi_1 a\zeta + \sum_{k=1}^{n} \phi_{2k+1}\left(1-\zeta^{2k}\right) a\zeta\right] \sin\theta \\ u_r &= \left[\psi_0 - \sum_{k=1}^{m} \psi_{2k} + \sum_{k=1}^{m} \psi_{2k}\left(1-\zeta^{2k}\right)\right] \sin\theta \\ u_\theta &= \left[\psi_0 - \sum_{k=1}^{m} \vartheta_{2k} + \sum_{k=1}^{m} \vartheta_{2k}\left(1-\zeta^{2k}\right)\right] \cos\theta\end{aligned} \tag{25}$$

- *Two-dimensional theories*:

$$\begin{aligned} u_x &= \left[\phi_1 a\zeta + \sum_{k=1}^{n} \phi_{2k+1}\left(1-\zeta^{2k}\right) a\zeta\right]\sin\theta \\ u_r &= \left[\psi_0 + \sum_{k=1}^{m} \psi_{2k}\left(1-\zeta^{2k}\right)\right]\sin\theta \\ u_\theta &= \left[\psi_0 + \sum_{k=1}^{m} \psi_{2k}\left(1-\zeta^{2k}\right)\right]\cos\theta \end{aligned} \tag{26}$$

- *One-dimensional theories*:

$$\begin{aligned} u_x &= \left[\phi_1 a\zeta + \sum_{k=1}^{n} \phi_{2k+1}\left(1-\zeta^{2k}\right) a\zeta\right]\sin\theta \\ u_r &= \psi_0 \sin\theta \\ u_\theta &= \psi_0 \cos\theta \end{aligned} \tag{27}$$

where the non-dimensional radius of the beam $\zeta$ is defined as $\zeta = r/a$, and where it was additionally assumed that the series representation of the longitudinal component $u_x$ may include $n$ terms, while in the case of two other directions $u_r$ and $u_\theta$ the number of the terms may be $m$.

Equations of motion associated with various theories of flexural behaviour of beam structural elements, based on the general forms of the displacement fields expressed by Eqs.(25)-(27), can be easily achieved, formulated and investigated by making use of the Hamilton's principle, as shown in details in [43] in the case of rod theories. It can be easily found out that appropriate selection of the terms $\phi_{2k+1}$, $\psi_{2k}$ and $\vartheta_{2k}$ leads to specific beam theories such as: single-mode Bernoulli-Rayleigh, two-mode Timoshenko or higher order two-mode Reddy theories. The theories presented below and analysed by the authors were classified as one-, two- and three-dimensional beam theories of flexural behaviour based on the nature of their stress and strain fields. Certain results of this classification are presented below together with dispersion curves for the group-to-phase velocity ratio $c_g/c_p$ in the case of selected beam theories, which illustrate Figs. 6-8.

It should be strongly emphasised once again that the number of wave propagation modes used by a particular theory of beam flexural behaviour presented below is always equivalent to the total number of degrees of freedom per node of a finite element formulated based on this theory.

**One-dimensional beam theories** ($\epsilon_{xx} \neq 0, \epsilon_{rr} = \epsilon_{\phi\phi} = 0$)

1. *Classical single-mode theory* (Bernoulli, Euler or Bernoulli-Euler):

$$\begin{gathered} n = 0, \quad \psi_0 \neq 0 \\ \tau_{xr} = 0 \rightarrow \phi_1 = -\frac{d\psi_0}{dx} \end{gathered} \tag{28}$$

noting that the contribution to the beam kinetic energy $T$ related to the longitudinal velocity $\dot{u}_x$ is neglected leading to:

$$T = \frac{\pi a^2 \rho}{2} \left(\dot{\psi}_0\right)^2$$

where $\dot{\square}$ denote the first time derivative.

2. *Single-mode Bernoulli-Rayleigh theory*:

$$\begin{gathered} n = 0, \quad \psi_0 \neq 0 \\ \tau_{xr} = 0 \rightarrow \phi_1 = -\frac{d\psi_0}{dx} \end{gathered} \tag{29}$$

where now the beam kinetic energy $T$ is expressed as:

$$T = \frac{\pi a^4 \rho}{8} \left(\frac{d\dot{\psi}_0}{dx}\right)^2 + \frac{\pi a^2 \rho}{2} \left(\dot{\psi}_0\right)^2$$

3. *Two-mode Timoshenko theory*:

$$n = 0, \quad \phi_1 \neq \psi_0 \neq 0 \tag{30}$$

4. *Higher order two-mode Reddy theory* – see Fig. 6:

$$\begin{gathered} n = 1, \quad \phi_1 \neq \psi_0 \neq 0 \\ \tau_{xr}|_{\zeta=1} = 0 \rightarrow \phi_3 = \frac{1}{2}\left(\phi_1 + \frac{d\psi_0}{dx}\right) \end{gathered} \tag{31}$$

5. *Three-mode theory*:

$$n = 1, \quad \phi_1 \neq \phi_3 \neq \psi_0 \neq 0 \tag{32}$$

6. *Higher order three-mode theory* – see Fig. 7:

$$n = 2, \quad \phi_1 \neq \phi_3 \neq \psi_0 \neq 0$$
$$\tau_{xr}|_{\zeta=1} = 0 \rightarrow \phi_5 = \frac{1}{4}\left(\phi_1 - 2\phi_3 + \frac{d\psi_0}{dx}\right) \tag{33}$$

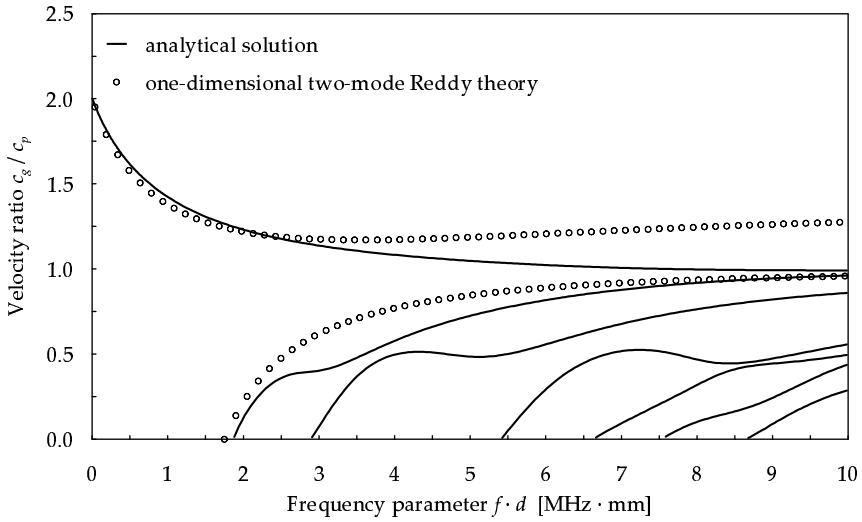


Fig. 6. Dispersion curves for the group-to-phase velocity ratio $c_g/c_p$ for the one-dimensional higher order two-mode Reddy theory of beams ($c_l = 6.3$ km/s, $c_t = 3.2$ km/s).

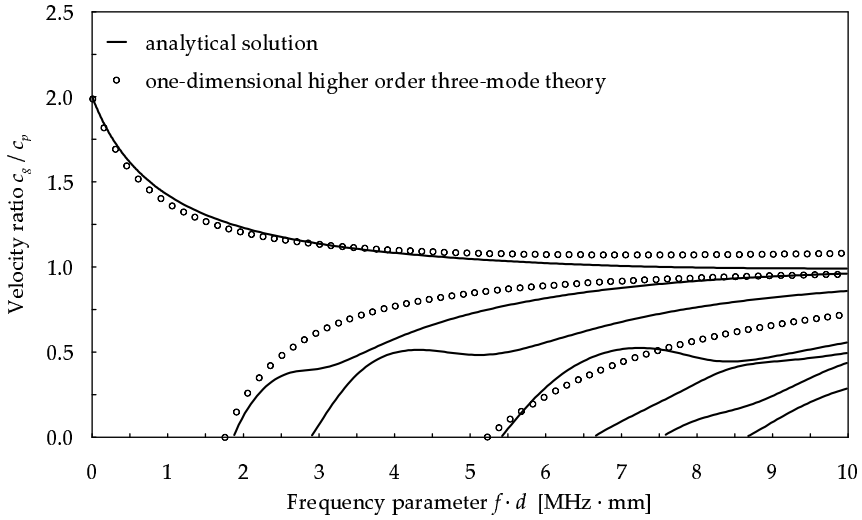


Fig. 7. Dispersion curves for the group-to-phase velocity ratio $c_g/c_p$ for the one-dimensional higher order three-mode theory of beams ($c_l = 6.3$ km/s, $c_t = 3.2$ km/s).

**Two-dimensional beam theories** ($\epsilon_{xx} \neq \epsilon_{rr} \neq 0, \epsilon_{\phi\phi} = 0$)

1. *Higher order two-mode theory*:

$$n = m = 1, \quad \phi_1 \neq \psi_0 \neq 0$$
$$\tau_{xr}|_{\zeta=1} = 0 \rightarrow \phi_3 = \frac{1}{2}\left(\phi_1 + \frac{d\psi_0}{dx}\right) \tag{34}$$
$$\sigma_{rr}|_{\zeta=1} = 0 \rightarrow \psi_2 = \frac{\lambda}{\lambda + 2\mu}\frac{a^2}{2}\frac{d\phi_1}{dx}$$

2. *Three-mode theory* – see Fig. 8:

$$n = 0, \quad m = 1, \quad \phi_1 \neq \psi_0 \neq \psi_2 \neq 0 \tag{35}$$

3. *Higher order three-mode theory A*:

$$n = 1, \quad m = 2, \quad \phi_1 \neq \psi_0 \neq \psi_2 \neq 0$$
$$\tau_{xr}|_{\zeta=1} = 0 \rightarrow \phi_3 = \frac{1}{2}\left(\phi_1 + \frac{d\psi_0}{dx}\right) \tag{36}$$
$$\sigma_{rr}|_{\zeta=1} = 0 \rightarrow \psi_4 = \frac{1}{2}\left(\frac{\lambda}{\lambda + 2\mu}\frac{a^2}{2}\frac{d\phi_1}{dx} - \psi_2\right)$$

4. *Higher order three-mode theory B*:

$$n = 2, \quad m = 1, \quad \phi_1 \neq \phi_3 \neq \psi_0 \neq 0$$
$$\tau_{xr}|_{\zeta=1} = 0 \rightarrow \phi_5 = \frac{1}{4}\left(\phi_1 - 2\phi_3 + \frac{d\psi_0}{dx}\right) \tag{37}$$
$$\sigma_{rr}|_{\zeta=1} = 0 \rightarrow \psi_2 = \frac{\lambda}{\lambda + 2\mu}\frac{a^2}{2}\frac{d\phi_1}{dx}$$

5. *Four-mode theory*:

$$n = m = 1, \quad \phi_1 \neq \phi_3 \neq \psi_0 \neq \psi_2 \neq 0 \tag{38}$$

6. *Higher order four-mode theory*:

$$n = m = 2, \quad \phi_1 \neq \phi_3 \neq \psi_0 \neq \psi_2 \neq 0$$

$$\tau_{xr}|_{\zeta=1} = 0 \rightarrow \phi_5 = \frac{1}{4}\left(\phi_1 - 2\phi_3 + \frac{d\psi_0}{dx}\right) \tag{39}$$

$$\sigma_{rr}|_{\zeta=1} = 0 \rightarrow \psi_4 = \frac{1}{2}\left(\frac{\lambda}{\lambda + 2\mu}\frac{a^2}{2}\frac{d\phi_1}{dx} - \psi_2\right)$$

7. *Five-mode theory A*:

$$n = 1, \quad m = 2, \quad \phi_1 \neq \phi_3 \neq \psi_0 \neq \psi_2 \neq \psi_4 \neq 0 \tag{40}$$

8. *Five-mode theory B*:

$$n = 2, \quad m = 1, \quad \phi_1 \neq \phi_3 \neq \phi_5 \neq \psi_0 \neq \psi_2 \neq 0 \tag{41}$$

9. *Six-mode theory* – see Fig. 9:

$$n = m = 2, \quad \phi_1 \neq \phi_3 \neq \psi_5 \neq \psi_0 \neq \psi_2 \neq \phi_4 \neq 0 \tag{42}$$

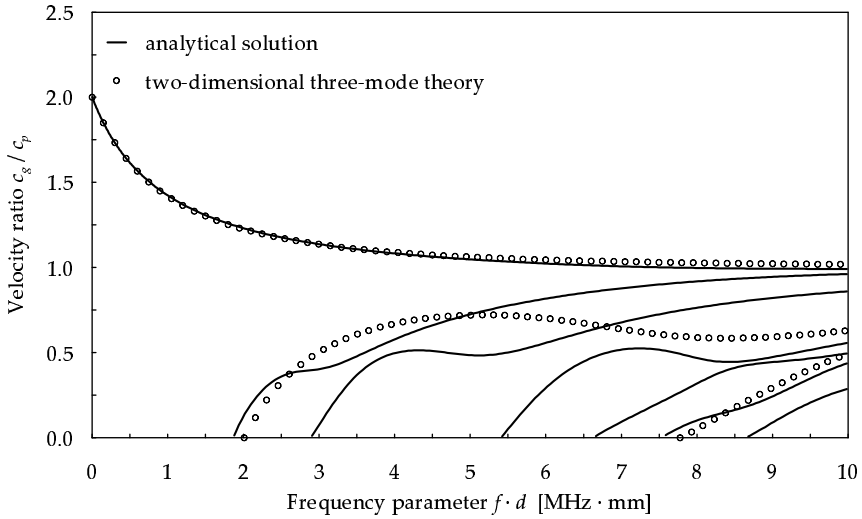


Fig. 8. Dispersion curves for the group-to-phase velocity ratio $c_g/c_p$ for the two-dimensional three-mode theory of beams ($c_l = 6.3$ km/s, $c_t = 3.2$ km/s).

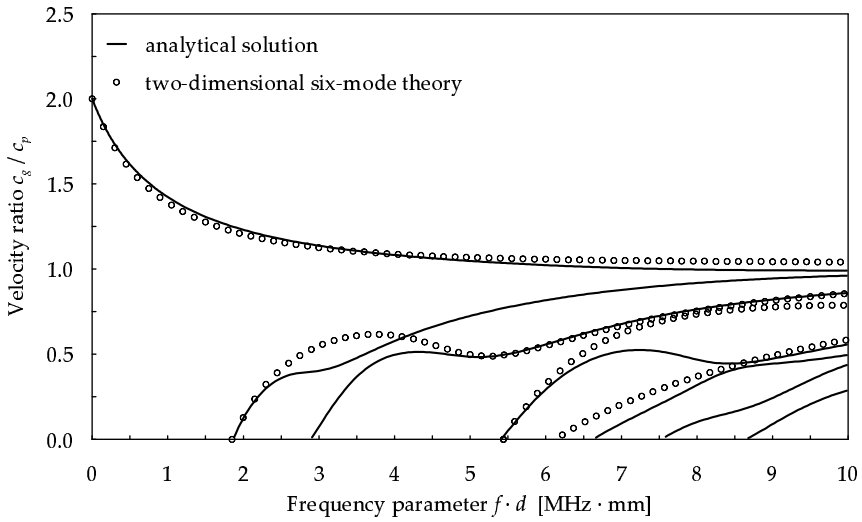


Fig. 9. Dispersion curves for the group-to-phase velocity ratio $c_g/c_p$ for the two-dimensional six-mode theory of beams ($c_l = 6.3$ km/s, $c_t = 3.2$ km/s).

---

**Three-dimensional beam theories** ($\epsilon_{xx} \neq \epsilon_{rr} \neq \epsilon_{\phi\phi} \neq 0$)

---

1. *Higher order two-mode theory*:

$$
\begin{gathered}
n = m = 1, \quad \phi_1 \neq \psi_0 \neq 0 \\
\tau_{r\theta}|_{\zeta=1} = 0 \rightarrow \vartheta_2 = -\psi_2 \\
\tau_{xr}|_{\zeta=1} = 0 \rightarrow \phi_3 = \frac{1}{2}\left(\phi_1 + \frac{d\psi_0}{dx} - \frac{d\psi_2}{dx}\right) \\
\sigma_{rr}|_{\zeta=1} = 0 \rightarrow \psi_2 = \frac{\lambda}{3\lambda + 4\mu}\left(\vartheta_2 + a^2 \frac{d\phi_1}{dx}\right)
\end{gathered}
\tag{43}
$$

2. *Higher order three-mode theory*:

$$
\begin{gathered}
n = 2, \quad m = 1, \quad \phi_1 \neq \phi_3 \neq \psi_0 \neq 0 \\
\tau_{r\theta}|_{\zeta=1} = 0 \rightarrow \vartheta_2 = -\psi_2 \\
\tau_{xr}|_{\zeta=1} = 0 \rightarrow \phi_5 = \frac{1}{4}\left(\phi_1 - 2\phi_3 + \frac{d\psi_0}{dx} - \frac{d\psi_2}{dx}\right) \\
\sigma_{rr}|_{\zeta=1} = 0 \rightarrow \psi_2 = \frac{\lambda}{3\lambda + 4\mu}\left(\vartheta_2 + a^2 \frac{d\phi_1}{dx}\right)
\end{gathered}
\tag{44}
$$

3. *Higher order four-mode theory*:

$$
\begin{gathered}
n=1, \quad m=2, \quad \phi_1 \neq \psi_0 \neq \psi_2 \neq \vartheta_2 \neq 0 \\
\tau_{r\theta}|_{\zeta=1}=0 \rightarrow \vartheta_4=-\frac{1}{3}\left(\psi_2+\psi_4+\vartheta_2\right) \\
\tau_{xr}|_{\zeta=1}=0 \rightarrow \phi_3=\frac{1}{2}\left(\phi_1+\frac{d\psi_0}{dx}-\frac{d\psi_2}{dx}-\frac{d\psi_4}{dx}\right) \\
\sigma_{rr}|_{\zeta=1}=0 \rightarrow \psi_4=-\frac{3\lambda+4\mu}{5\lambda+8\mu}\psi_2+\frac{\lambda}{5\lambda+8\mu}\left(\vartheta_2+\vartheta_4+a^2\frac{d\phi_1}{dx}\right)
\end{gathered}
\tag{45}
$$

4. *Five-mode theory*:

$$
n=m=1, \quad \phi_1 \neq \phi_3 \neq \psi_0 \neq \psi_2 \neq \vartheta_2 \neq 0 \tag{46}
$$

5. *Higher order five-mode theory* – see Fig. 10:

$$
\begin{gathered}
n=m=2, \quad \phi_1 \neq \phi_3 \neq \psi_0 \neq \psi_2 \neq \vartheta_2 \neq 0 \\
\tau_{r\theta}|_{\zeta=1}=0 \rightarrow \vartheta_4=-\frac{1}{3}\left(\psi_2+\psi_4+\vartheta_2\right) \\
\tau_{xr}|_{\zeta=1}=0 \rightarrow \phi_3=\frac{1}{4}\left(\phi_1-2\phi_2+\frac{d\psi_0}{dx}-\frac{d\psi_2}{dx}-\frac{d\psi_4}{dx}\right) \\
\sigma_{rr}|_{\zeta=1}=0 \rightarrow \psi_4=-\frac{3\lambda+4\mu}{5\lambda+8\mu}\psi_2+\frac{\lambda}{5\lambda+8\mu}\left(\vartheta_2+\vartheta_4+a^2\frac{d\phi_1}{dx}\right)
\end{gathered}
\tag{47}
$$

6. *Six-mode theory*:

$$
n=2, \quad m=1, \quad \phi_1 \neq \phi_3 \neq \phi_5 \neq \psi_0 \neq \psi_2 \neq \vartheta_2 \neq 0 \tag{48}
$$

7. *Seven-mode theory*:

$$
n=1, \quad m=2, \quad \phi_1 \neq \phi_3 \neq \psi_0 \neq \psi_2 \neq \psi_4 \neq \vartheta_2 \neq \vartheta_4 \neq 0 \tag{49}
$$

8. *Eight-mode theory* – see Fig. 11:

$$
n=m=2, \quad \phi_1 \neq \phi_3 \neq \phi_5 \neq \psi_0 \neq \psi_2 \neq \psi_4 \neq \vartheta_2 \neq \vartheta_4 \neq 0 \tag{50}
$$

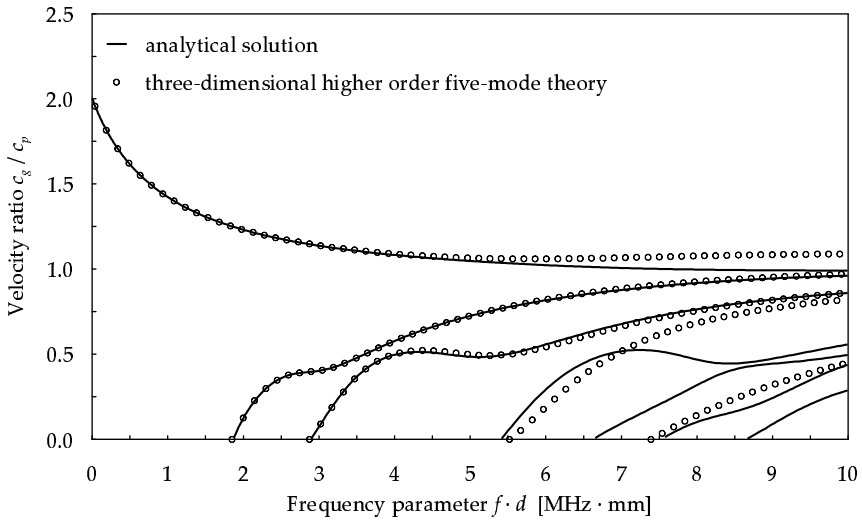


Fig. 10. Dispersion curves for the group-to-phase velocity ratio $c_g/c_p$ for the three--dimensional higher order five-mode theory of beams ($c_l = 6.3$ km/s, $c_t = 3.2$ km/s).

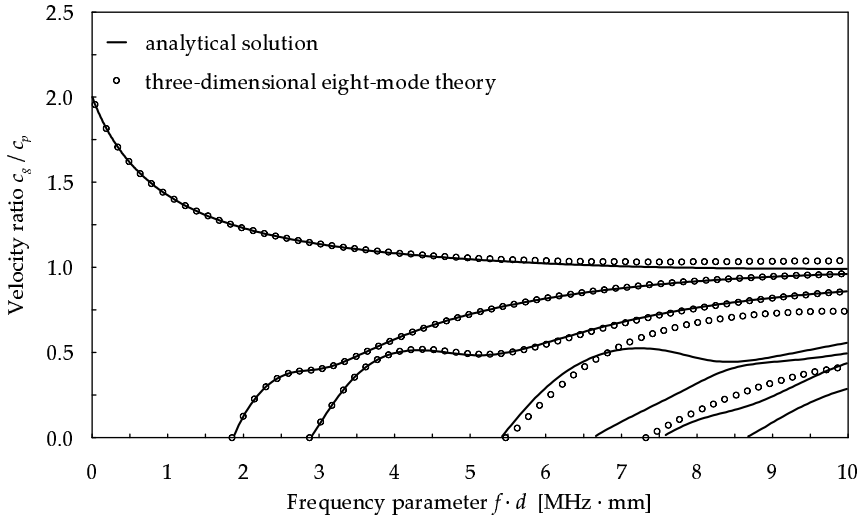


Fig. 11. Dispersion curves for the group-to-phase velocity ratio $c_g/c_p$ for the three--dimensional eight-mode theory of beams ($c_l = 6.3$ km/s, $c_t = 3.2$ km/s).

### *3.3 Comparison of beam theories*

Particular one-, two- or three-dimensional theories of beam flexural behaviour employed to study and investigate various dynamic problems, or problems related to propagation of elastic flexural (bending) waves, can be characterised by many factors, in which their accuracy and their costs of numerical implementation seem to be the most crucial ones. The accuracy of various beam theories may assessed in many different ways. The authors of this work propose to use for that purpose a method based on dispersion curves associated with the theories investigated within a certain frequency range of interest. This fre-

quency range may be different and in special cases may cover propagation of one, two or even more modes of flexural waves. This is very well illustrated by Figs. 6-11 showing dispersion curves obtained for the group-to-phase velocity ratio $c_g/c_p$ for selected one-, two- and three-dimensional theories of beam flexural behaviour, presented and discussed in the previous section of this paper. For majority of practical applications, however, the range of the frequency parameter $f \cdot d$ usually covers propagation of the first flexural mode up to the first cut-off frequency $f_a$ or alternatively may include propagation of the second flexural mode up to the second cut-off frequency $f_b$. In the case of the beam made out of aluminium and already considered the corresponding values of the frequency parameter $f \cdot d$ are equal to $f_a \cdot d = 1.88$ MHz· mm or $f_b \cdot d = 2.91$ MHz· mm, respectively.

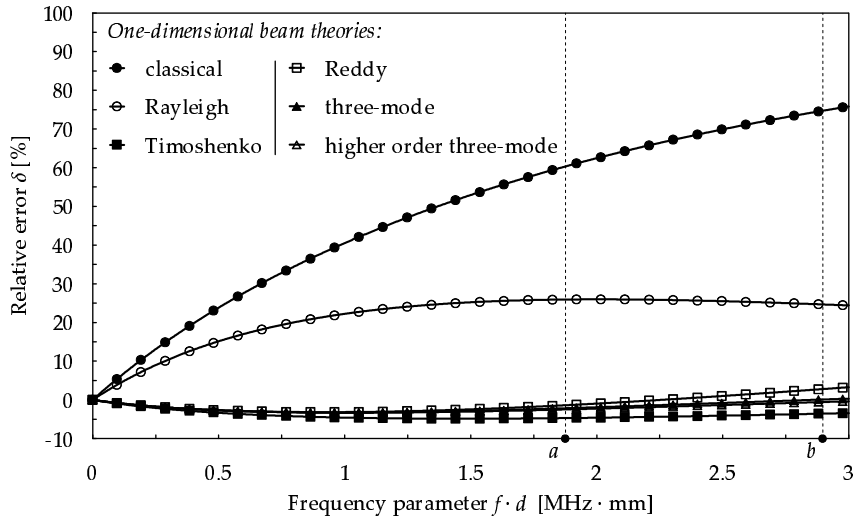


Fig. 12. Relative errors for various one-dimensional theories of beam flexural behaviour measured against the analytical solution for the fundamental propagation mode ($c_l = 6.3$ km/s, $c_t = 3.2$ km/s).

In order to investigate the theories of beam flexural behaviour presented and discussed in this paper the range of the frequency parameter $f \cdot d$ was limited to 3.0 MHz· mm, while the assessment was restricted to the fundamental flexural mode. In the case of particular one-, two- and three-dimensional beam theories a relative error $\delta$ was evaluated based on the dispersion curve for the group-to-phase velocity ratio $c_g/c_p$ for the fundamental flexural mode calculated based on the assessed theory and the corresponding dispersion curve calculated based on the analytical solution given by Eq. (15):

$$\delta = \frac{r_\beta - r_\alpha}{r_\alpha} \times 100\%, \quad r_i = \left.\frac{c_g}{c_p}\right|_i, \quad i = \alpha, \beta \tag{51}$$

where now $r_i$ is the group-to-phase velocity ratio $c_g/c_p$, with $i = \alpha, \beta$, and where $r_\alpha$ denotes the ratio calculated based on the analytical solution and $r_\beta$

is the same ratio calculated based on particular beam theories.

The results obtained were grouped and presented in Figs. 12-14 for one-, two- or three-dimensional theories of beam flexural behaviour, where points $a$ and $b$ in the figures correspond to the first cut-off frequency $f_a \cdot d$ and the second cut-off frequency $f_b \cdot d$, respectively.

It can seen from Fig. 12 that in the case of the one-dimensional theories of beam flexural behaviour, within the given range of the frequency parameter $f \cdot d$, the higher order two-mode Reddy theory is characterised by the smallest magnitude of the relative error $\delta$ reaching -3.2% at 0.92 MHz· mm. On the other hand the classical single-mode theory is characterised by the highest magnitude of the error $\delta$ increasing gradually to 75.8% at 3.0 MHz· mm.

It is very interesting to note that the remaining higher order and/or higher-mode theories offer no increased accuracy in comparison to the higher order two-mode Reddy theory. This unexpected behaviour may be attributed to the fact that the higher order terms of the series expansion, included in the displacement field given by Eqs. 27 and restricted only to the longitudinal displacement component $u_x$, are insufficient to support any increase in the accuracy, since predominant effects have the errors resulting from neglecting the real three-dimensional nature of the strain field.

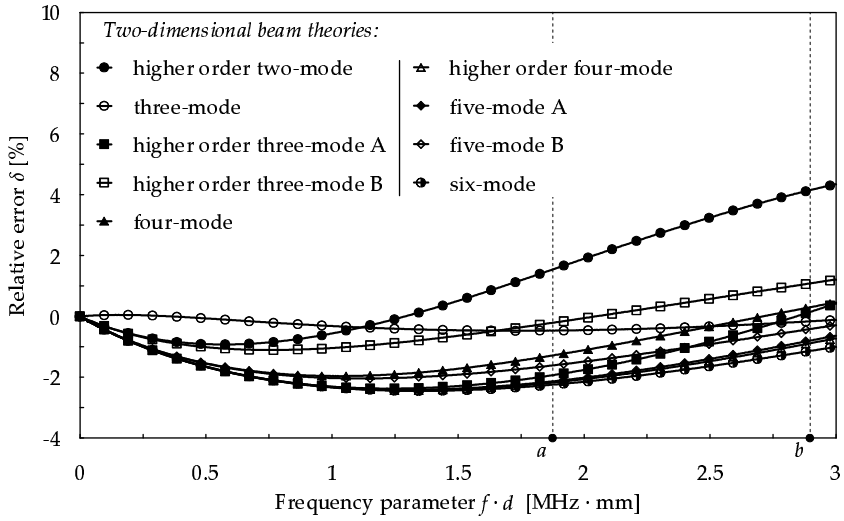


Fig. 13. Relative errors for various two-dimensional theories of beam flexural behaviour measured against the analytical solution for the fundamental propagation mode ($c_l = 6.3$ km/s, $c_t = 3.2$ km/s).

A very similar kind of behaviour can be observed from Fig. 13 in the case of two-dimensional theories of beam flexural behaviour. In general these theories are characterised by much smaller magnitudes of the relative error $\delta$ than the one-dimensional theories. Out of the theories investigated the three-mode the-

ory is characterised by the smallest magnitude of the relative error $\delta$ reaching 0.5% at 0.14 MHz· mm. On the other hand the higher order two-mode theory is characterised by the highest magnitude of the error $\delta$ exceeding 4.3% at 3.0 MHz· mm. As before this unusual behaviour has the same origins as in the case of the one-dimensional theories, however, it is very interesting to note that for the two-dimensional theories assessed now the higher order terms of the series expansion, included in the displacement field given by Eqs. 26 for the radial displacement component $u_r$, have greater effects than the corresponding terms associated with the longitudinal displacement component $u_x$. This is clearly seen for the higher order three-mode theories A and B as well as the five-mode theories A and B.

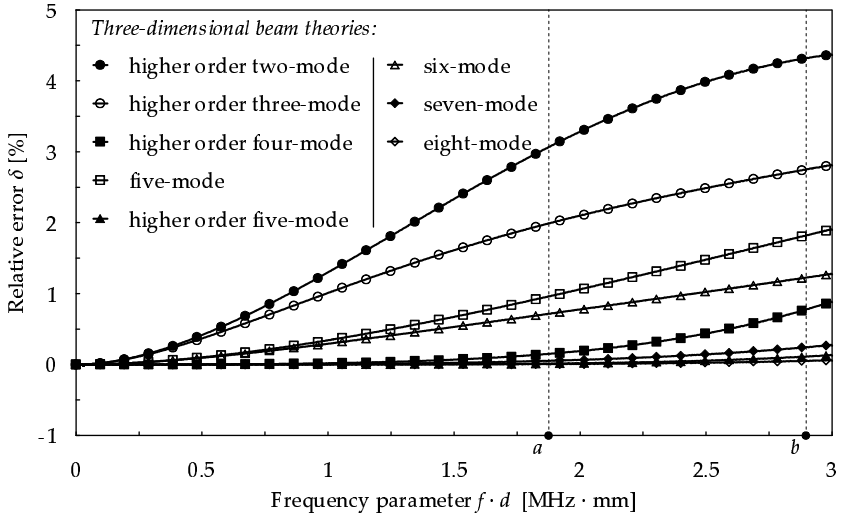


Fig. 14. Relative errors for various three-dimensional theories of beam flexural behaviour measured against the analytical solution for the fundamental propagation mode ($c_l = 6.3$ km/s, $c_t = 3.2$ km/s).

In the case of the three-dimensional theories of beam flexural behaviour shown in Fig. 14 the observed trend is different. It can be noticed that the higher order and/or higher-mode theories presented are always characterised by improved accuracy in comparison to all lower-mode theories analysed. This is a direct consequence of the fact that the three-dimensional theories make no oversimplifying assumptions related to the three-dimensional nature of the strain field. For this reason additional higher order terms of the series expansion, included in the displacement field given by Eqs. 25, always contribute to an increase in the accuracy, which is clearly observed in Fig. 14. Out of the theories investigated here the eight-mode theory is characterised by the smallest magnitude of the relative error $\delta$ reaching 0.06% at 3.0 MHz· mm, while at the same time the highest magnitude of the relative error $\delta$ reaching 4.4% at 3.0 MHz· mm is associated with the higher-order two-mode theory.

In order to estimate the numerical costs of the one-, two- or three-dimensional

Table 1
Comparison of various theories of beam flexural behaviour discussed in the text.

| **One-dimensional beam theories** ($\epsilon_{xx} \neq 0, \epsilon_{rr} = \epsilon_{\phi\phi} = 0$) | | | | | | |
|---|---|---|---|---|---|---|
| *beam theory* | $I_1^a[\%]$ | $I_2^a[\%]$ | $I_1^b[\%]$ | $I_2^b[\%]$ | $I_3^a[\%]$ | $I_3^b[\%]$ |
| classical single-mode | 36.1 | 17.1 | 47.4 | 20.8 | 11.6 | 14.5 |
| single-mode Bernoulli-Rayleigh | 18.9 | 7.17 | 21.3 | 6.58 | 5.20 | 5.03 |
| two-mode Timoshenko | 3.85 | 1.30 | 3.97 | 1.07 | 3.88 | 3.38 |
| two-mode Reddy | 2.40 | 0.76 | 1.95 | 0.97 | 2.31 | 2.60 |
| three-mode | 2.59 | 0.76 | 2.04 | 1.04 | 5.28 | 6.20 |
| higher order three-mode | 2.68 | 0.78 | 2.27 | 0.90 | 5.45 | 5.82 |
| **Two-dimensional beam theories** ($\epsilon_{xx} \neq \epsilon_{rr} \neq 0, \epsilon_{\phi\phi} = 0$) | | | | | | |
| *beam theory* | $I_1^a[\%]$ | $I_2^a[\%]$ | $I_1^b[\%]$ | $I_2^b[\%]$ | $I_3^a[\%]$ | $I_3^b[\%]$ |
| higher order two-mode | 0.66 | 0.35 | 1.47 | 1.22 | 0.91 | 2.66 |
| three-mode | 0.26 | 0.18 | 0.29 | 0.16 | 0.94 | 0.91 |
| higher order three-mode A | 1.85 | 0.62 | 1.55 | 0.73 | 4.18 | 4.48 |
| higher order three-mode B | 0.77 | 0.30 | 0.67 | 0.34 | 1.92 | 2.02 |
| four-mode | 1.53 | 0.47 | 1.19 | 0.64 | 5.78 | 6.67 |
| higher order four-mode | 1.90 | 0.65 | 1.79 | 0.59 | 7.77 | 7.12 |
| five-mode A | 1.89 | 0.64 | 1.75 | 0.60 | 12.0 | 11.1 |
| five-mode B | 1.62 | 0.51 | 1.41 | 0.54 | 9.67 | 9.77 |
| six-mode | 1.92 | 0.66 | 1.85 | 0.57 | 17.7 | 15.8 |
| **Three-dimensional beam theories** ($\epsilon_{xx} \neq \epsilon_{rr} \neq \epsilon_{\phi\phi} \neq 0$) | | | | | | |
| *beam theory* | $I_1^a[\%]$ | $I_2^a[\%]$ | $I_1^b[\%]$ | $I_2^b[\%]$ | $I_3^a[\%]$ | $I_3^b[\%]$ |
| higher order two-mode | 1.29 | 0.97 | 2.18 | 1.45 | 2.22 | 3.49 |
| higher order three-mode | 0.94 | 0.64 | 1.45 | 0.88 | 3.41 | 4.93 |
| higher order four-mode | 0.03 | 0.04 | 0.17 | 0.21 | 0.30 | 1.49 |
| five-mode | 0.37 | 0.29 | 0.73 | 0.57 | 4.08 | 7.96 |
| higher order five-mode | 0.00 | 0.00 | 0.02 | 0.03 | 0.04 | 0.30 |
| six-mode | 0.30 | 0.22 | 0.54 | 0.38 | 4.57 | 8.01 |
| seven-mode | 0.01 | 0.01 | 0.06 | 0.07 | 0.34 | 1.49 |
| eight-mode | 0.00 | 0.00 | 0.01 | 0.01 | 0.06 | 0.36 |

theories of beam flexural behaviour investigated in this work it is necessary to identify a certain averaged indicator that could be capable to characterise the theories and that should take into account not only their accuracy but also the multimode nature of the theories. The authors propose to built it as based on three other indicators averaging the relative error $\delta$ as well as averaging its variation within the chosen range of the frequency parameter $f \cdot d$, in the current case limited to 3.0 MHz· mm. They are defined as follows:

$$
\begin{aligned}
I_1^i &= \frac{1}{x_i} \int_0^{x_i} |\delta(x)| \, \mathrm{d}x \\
I_2^i &= \sqrt{\frac{1}{x_i} \int_0^{x_i} \{|\delta(x)| - I_1^i\}^2 \, \mathrm{d}x} \\
I_3^i &= \frac{I_1^i I_2^i}{I_1^i + I_2^i} \, n^2
\end{aligned}
\tag{52}
$$

where $n$ is the total number of modes used by the theories, while $x_i = f_i \cdot d$, with $i = a, b$, denotes the values of the frequency parameter corresponding to the first cut-off frequency $f_a \cdot d$ or the second cut-off frequency $f_b \cdot d$, respectively. It can be noticed that the indicator $I_3^i$ as proportional to the square of the mode number $n$ indicates not only the averaged accuracy of the beam theories assessed, but it also reflects the cost of computer memory usage required to store the characteristic matrices of beam elements based on these theories.

The results presented in Table 1 clearly indicate that out of all one-, two- and three-dimensional theories of beam flexural behaviour investigated the three-dimensional higher order five-mode theory is characterised by the smallest, near to zero, values of the indicator $I_3^a$ and $I_3^b$ equal to 0.04% and 0.3%, in both the ranges of the frequency parameter $f \cdot d$. Similar results were obtained for the three-dimensional eight-mode theory and also in the case of the two-dimensional three-mode theory. However in those two cases the values of the indicators $I_3^a$ and $I_3^b$ are greater and equal to 0.06% and 0.36% as well as to 0.94% and 0.91%, respectively. It is very interesting to note that the one-dimensional theories, despite their relative simplicity of practical implementation, offer degrees of accuracy much lower than more demanding in that respect two- or even three-dimensional theories. In the best case of the higher order two-mode Reddy theory the values of the indicators $I_3^a$ and $I_3^b$ are as high as 2.31% and 2.6%. As a consequence of that the errors resulting from the application of simplified theories may mask very important and relevant information that otherwise could be revealed if only two- or three-dimensional theories of beam flexural behaviour were used instead.

## 4 Conclusions

In this work different theories of beam flexural behaviour have been discussed and compared that are commonly used to investigate beam behaviour associated with dynamics or propagation of flexural elastic waves. This includes various one-, two- and three-dimensional theories comprising the classical one-dimensional Bernoulli, Bernoulli-Rayleigh, Timoshenko and Reddy theories, as well as various higher order and/or higher-mode theories of beam flexural behaviour developed by the authors.

Based on the results presented in this work certain general conclusions can be drawn:

1. One-dimensional theories of beam flexural behaviour, due to their relative simplicity, offer the worst accuracy in a broad range of frequencies. This problem becomes very important for high frequency regimes, as is propagation of flexural elastic waves. For this reason one-dimensional theories may be effectively used in the case of static or low-frequency dynamic problems.

2. Two-dimensional theories of beam flexural behaviour offer an increased level of accuracy in comparison to the one-dimensional theories at the cost of their increased complexity, however, this is true only in the case of lower-mode theories. Because of the same reasons two-dimensional theories may be successfully applied in the case of static or low-to-medium frequency dynamic problems.

3. It should be strongly emphasised that all higher order and/or higher-mode one- and two-dimensional theories of beam flexural behaviour suffer from fall in their accuracy with enrichment of their displacement field by higher order terms of the series expansion of the fully three-dimensional displacement field. This is a direct consequence of their inability to mimic the real three-dimensional nature of the strain field associated with propagation of elastic flexural waves.

4. Three-dimensional theories of beam flexural behaviour are characterised by superior accuracy at their moderate complexity. They can be successfully applied for all types of dynamic problems including propagation of elastic flexural waves in wide ranges of frequencies. Moreover, higher order and/or higher-mode theories always offer improved accuracy in comparison to lower-mode theories.

5. Special attention should be paid for all these problems that concern very high-frequency dynamics and are related with simultaneous propagation of multiple modes of flexural waves. In all such case the accuracy of the beam theory applied should be always individually assessed, however, it is recommended

by the authors that higher order and/or higher-mode three-dimensional theories are used for that purpose.

6. It should be noted that the development and subsequent application of higher order higher-mode theories of beam flexural behaviour is relatively simple in the case of isotropic materials. Despite its complexity in a more general circumstances of anisotropic materials the same methodology can be adopted. Unfortunately all resulting relations are much more complicated mathematically therefore it is recommended by the authors to use higher-mode theories of in all such cases.

## References


[1] S. Timoshenko: *History of strength of materials.* Dover Publications, 1983.

[2] J. W. S. Rayleigh: *The theory of sound.* Macmillan and Co., London, 1877.

[3] S. Timoshenko: *On the correction factor for shear of the differential equation for transverse vibrations of bars of uniform cross-section.* Philosophical Magazine Series 6, **41**, 744-746, 1921.

[4] S. Timoshenko: On the transverse vibrations of bars of uniform cross-section. Philosophical Magazine Series 6, **43**, 125-131, 1922.

[5] M. Levinson: *A new rectangular beam theory.* Journal of Sound and Vibration, **74**, 81-87, 1981.

[6] P. R. Heyliger, J. N. Reddy: *A higher-order beam finite element for bending and vibration problems.* Journal of Sound and Vibration, **126**, 309-326, 1988.

[7] V. Z. Vlasov: *Thin-walled elastic beams.* Israel Program for Scientific Translations, Jerusalem, 1961.

[8] W. Yu, D. H. Hodgesb, V. V. Volovoib, E. D. Fuchs: *A generalized Vlasov theory for composite beams.* Thin-Walled Structures, **43**. 1493-1511, 2005.

[9] C. Kim, S. R. White: *Thick-walled composite beam theory including 3-d elastic effects and torsional warping.* International Journal of Solids and Structures, **34**, 4237-4259, 1997.

[10] B. Saint-Venant: *Mémoire sur la torsion des prismes.* Mémoires des Savants Étrangers, **14**, 233-560, 1855.

[11] B. Saint-Venant: *Mémoire sur la flexion des prismes.* Journal de Mathématiques de Liouville, **1**, 89-189, 1856.

[12] J. F. Doyle: *Wave propagation in structures.* Springer-Verlag New York Inc., New York, 1997.

[13] D. Roy Mahapatra, S. Gopalakrishnan: *Spectral-element-based solutions for wave propagation analysis of multiply connected unsymmetric lami-*

*nated composite beams.* Journal of Sound and Vibration, **237**, 819-836, 2000.

[14] M. Krawczuk, M. Palacz, W. Ostachowicz: *The dynamic analysis of a cracked Timoshenko beam by the spectral element method.* Journal of Sound and Vibration, **264**, 1139-1153, 2003.

[15] M. Krawczuk, A. Żak, W. Ostachowicz, M. Cartmell: *Propagation of elastic waves in beams - including damping effects.* Materials Science Forum, **440-441**, 179-186, 2003.

[16] M. Krawczuk, M. Palacz, W. Ostachowicz: *Flexural-shear wave propagation in cracked composite beam.* Science and Engineering of Composite Materials, **11**, 55-67, 2004.

[17] D. Sreekanth Kumar, D. Roy Mahapatra, S. Gopalakrishnan: *A spectral finite element for wave propagation and structural diagnostic analysis of composite beam with transverse crack.* Finite Elements in Analysis and Design, **40**, 1729-1751, 2004.

[18] W. Ostachowicz, M. Krawczuk, M. Cartmell, M. Gilchrist: *Wave propagation in delaminated beam.* Computers and Structures, **82**, 475-483, 2004.

[19] M. Palacz, M. Krawczuk. W. Ostachowicz: *The spectral finite element model for analysis of flexural-shear coupled wave propagation. Part 1: Laminated multilayer composite beam.* Composite Structures, **68**, 37-44, 2005.

[20] M. Palacz, M. Krawczuk, W. Ostachowicz: *The spectral finite element model for analysis of flexural-shear coupled wave propagation. Part 2: Delaminated multilayer composite beam.* Composite Structures, **68**, 45-51, 2005.

[21] A. Chakraborty: *Wave propagation in anisotropic poroelastic beam with axial-flexural coupling.* Computational Mechanics, **43**, 755-767, 2009.

[22] S. M. Choo, S. K.Chung: *Finite difference approximate solutions for the strongly damped extensible beam equations.* Applied Mathematics and Computation, **112**, 11-32, 2000.

[23] F.-L. Li, Z.-Z. Sun: *A finite difference scheme for solving the Timoshenko beam equations with boundary feedback.* Computational and Applied Mathematics, **200**, 606-627, 2007.

[24] R. Ansari, R. Gholamia, K. Hosseini, S. Sahmania: *A sixth-order compact finite difference method for vibrational analysis of nanobeams embedded in an elastic medium based on nonlocal beam theory.* Mathematical and Computer Modelling, **54**, 2577-2586, 2011.

[25] J. Awrejcewicz, A. V. Krysko, J. Mrozowski, O. A. Saltykova, M. V. Zhigalov: *Analysis of regular and chaotic dynamics of the Euler-Bernoulli beams using finite difference and finite element methods.* Acta Mechanica Sinica, **27**, 36-43, 2011.

[26] S. R. Marur, T. Kant: *Free vibration analysis of fiber reinforced composite beams using higher order theories and finite element modelling.* Journal of Sound and Vibration, **194**, 337-351, 1996.

[27] M. Krawczuk, W. Ostachowicz: *Natural vibrations of a clamped-clamped arch with an open transverse crack.* ASME Journal of Vibration and Acoustics, **119**, 145-151, 1997.

[28] G. Shi, K. Y. Lam: *Finite element vibration analysis of composite beams based on higher-order beam theory.* Journal of Sound and Vibration, **219**, 707-721, 1999.

[29] S. Han, H. Benaroya, T. Wei: *Dynamics of transversely vibrating beams using four engineering theories.* Journal of Sound and Vibration, **225**, 935-988, 1999.

[30] A. Chakraborty, D. Roy Mahapatra, S. Gopalakrishnan: *Finite element analysis of free vibration and wave propagation in asymmetric composite beams with structural discontinuities.* Composite Structures, **55**, 23-36, 2002.

[31] A. T. Patera: *A spectral element method for fluid dynamics: Laminar flow in a channel expansion.* Journal of Computational Physics, **54**, 468-488, 1984.

[32] W. Ostachowicz, M. Krawczuk, A. Żak, P. Kudela: *Damage detection in elements of structures by the elastic wave propagation method.* Computer Assisted Mechanics and Engineering Sciences, **13**, 109-124, 2006.

[33] P. Kudela, M. Krawczuk, W. Ostachowicz: *Wave propagation modelling in 1D structures using spectral finite elements.* Journal of Sound and Vibration, **300**, 88-100, 2007.

[34] M. Krawczuk, M. Palacz, A. Żak, W. Ostachowicz: *Transmission and reflection coefficients for damage identification in 1D elements.* Key Engineering Materials, **413-414**, 95-100, 2009.

[35] M. Rucka: *Experimental and numerical study on damage detection in an L-joint using guided wave propagation.* Journal of Sound and Vibration, **329**, 1760-1779, 2010.

[36] J. Tian, Z. Li, X. Su: *Crack detection in beams by wavelet analysis of transient flexural waves.* Journal of Sound and Viration, **261**, 715-727, 2003.

[37] M. Mitra, S. Gopalakrishnan: *Spectrally formulated wavelet finite element for wave propagation and impact force identification in connected 1-D waveguides.* International Journal of Solids and Structures, **42**, 4695-4721, 2005.

[38] M. Mitra, S. Gopalakrishnan: *Wavelet based spectral finite element for analysis of coupled wave propagation in higher order composite beams.* Composite and Structures, **73**, 263-277, 2006.

[39] J. D. Achenbach: *Wave propagation in elastic solids.* North-Holland Publishing Company, Amsterdam, 1973.

[40] J. L. Rose: *Ultrasonic waves in solid media.* Cambridge University Press, Cambridge, 1999.

[41] `<URL: http://http://www.mathworks.com>`

[42] A. Ralston: *A first course in numerical analysis.* McGraw-Hill Book Company, New York, 1965.

[43] A. Żak, M. Krawczuk: *Assessment of rod behaviour theories used is spectral finite element modelling.* Journal of Sound and Vibration, **329**, 2099-2113, 2010.